

pubs.acs.org/JPCL Letter

# Mapping H<sup>+</sup> in the Nanoscale (A<sub>2</sub>C<sub>4</sub>)<sub>2</sub>-Ag<sub>8</sub> Fluorophore

Fred David, Caleb Setzler, Alexandra Sorescu, Raquel L. Lieberman, Flora Meilleur,\* and Jeffrey T. Petty\*



Cite This: J. Phys. Chem. Lett. 2022, 13, 11317-11322



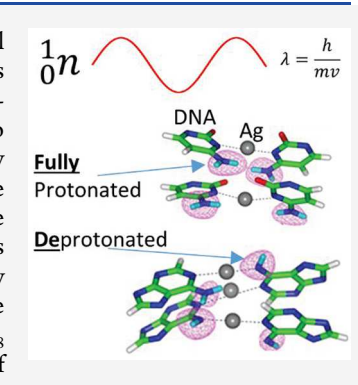
**ACCESS** I

Metrics & More

Article Recommendations

Supporting Information

**ABSTRACT:** When strands of DNA encapsulate silver clusters, supramolecular optical chromophores develop. However, how a particular structure endows a specific spectrum remains poorly understood. Here, we used neutron diffraction to map protonation in  $(A_2C_4)_2$ -Ag<sub>8</sub>, a greenemitting fluorophore with a "Big Dipper" arrangement of silvers. The DNA host has two substructures with distinct protonation patterns. Three cytosines from each strand collectively chelate handle-like array of three silvers, and calorimetry studies suggest Ag<sup>+</sup> cross-links. The twisted cytosines are further joined by hydrogen bonds from fully protonated amines. The adenines and their neighboring cytosine from each strand anchor a dipper-like group of five silvers via their deprotonated endo- and exocyclic nitrogens. Typically, exocyclic amines are strongly basic, so their acidification and deprotonation in  $(A_2C_4)_2$ -Ag<sub>8</sub> suggest that silvers perturb the electron distribution in the aromatic nucleobases. The different protonation states in  $(A_2C_4)_2$ -Ag<sub>8</sub> suggest that atomic level structures can pinpoint how to control and tune the electronic spectra of these nanoscale chromophores.



Trands of DNA are templates for molecularly sized silver clusters with ~10 atoms, and such DNA-cluster complexes are chromophores that are more akin to organic dyes than metal nanomaterials.<sup>1,2</sup> The clusters have sparsely organized valence electronic states that favor radiative electronic relaxation, as their excited states efficiently emit with  $\lesssim$ 90% quantum yields and  $\lesssim$ 10 ns lifetimes.<sup>3–5</sup> Alone, such metallic clusters are unstable but can be encapsulated and thus protected by oligonucleotides, and the now robust conjugates survive in aqueous buffers and biological media. 6,7 These composite chromophores are functional optical reporters because a DNA not only protects but also tunes its cluster adduct. The DNA sequence controls the cluster size and shape and thereby encodes the cluster spectra, which span the violet to near-infrared window. 8,9 Furthermore, the DNA secondary structure can be switched between single- and double-stranded forms to toggle the cluster brightness over an ~2000-fold range. 10,11 On the basis of this spectral and intensity control, DNA-based silver clusters have been developed as fluorescent labels and sensors for a wide range of biological and chemical targets. 12-14

The structure of nanoscale silver complexes guides the rational synthesis of specific chromophores. The point of the DNA-silver chromophores  $(A_2C_4)_2$ -Ag<sub>8</sub> and  $(CACCTGC-GA)_2$ -Ag<sub>16</sub>, three types of bonds have been identified via atomic resolution structures: 18-20 (1) Silvers coalesce into clusters, with metal-like bond distances of 2.6-2.9 Å. Their loosely bound 5s valence electrons are responsible for the spectra and chemical reactivity of these clusters. The electron-rich heteroatoms in the DNA nucleobases coordinate both Ag<sup>0</sup> and Ag<sup>+</sup>, and the collective set of

nucleobases in a strand define the binding site for a specific cluster.<sup>5,26,27</sup> (3) The nucleobase heteroatoms are not only Lewis bases that bind silvers but also Brønsted—Lowry acids and bases.<sup>28</sup> Proximal nucleobases can hydrogen bond, thereby joining and folding the DNA host. Hydrogen ions, which are the smallest structural element in these complexes, are not observed in cryogenic X-ray crystallography studies, but protonation in DNA-bound silver clusters is intimately linked with silver cluster spectra.<sup>29,30</sup>

Here, we combine neutron and X-ray diffraction to map the network of hydrogen bonds within the green fluorescent DNA-silver cluster complex  $(A_2C_4)_2$ -Ag<sub>8</sub>. Earlier X-ray diffraction studies at cryogenic temperatures showed that the two strands line up with parallel  $5' \rightarrow 3'$  orientations to form a [AACCCC]<sub>2</sub> duplex, and two binding sites develop for the 8 silvers, arranged like the stars in the Big Dipper asterism (Figure 1A). The lagging three cytosines in each strand arrange the remaining three silvers into an extended, handle-like shape. The two leading adenines and their neighboring cytosine together bind five of the silvers with a trapezoidal, dipper-like shape and metal-like bonds. In these studies, complementary room-temperature X-ray and neutron diffraction studies distinguish protonation patterns in the handle and dipper substructures of the  $(A_2C_4)_2$ -Ag<sub>8</sub> fluorophore. More broadly,

Received: October 17, 2022 Accepted: November 22, 2022 Published: December 1, 2022





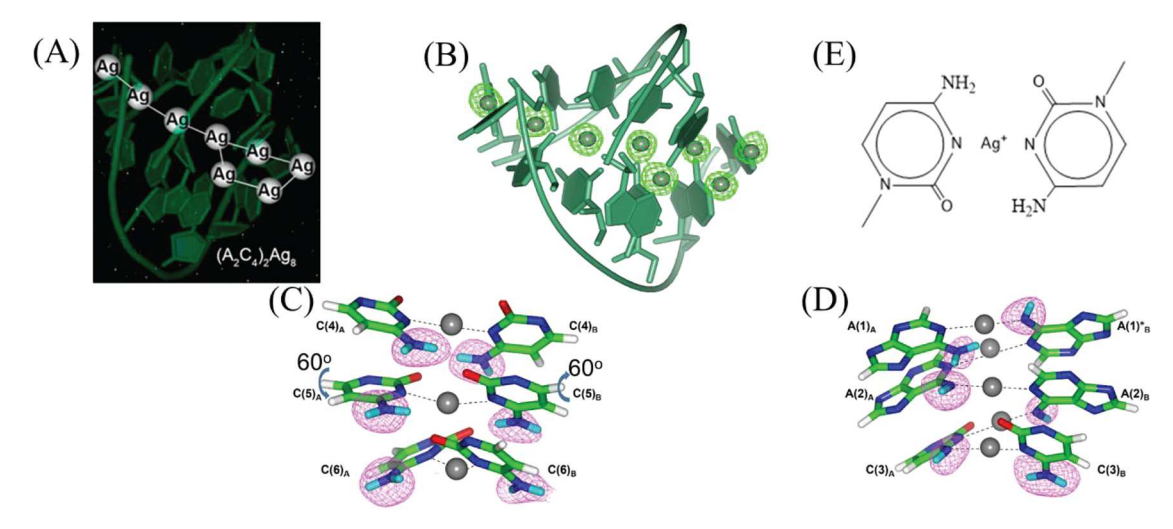


Figure 1. Arrangement of Ag and H atoms in  $(A_2C_4)_2$ -Ag<sub>8</sub>. (A, B) Two views of the silver organization in the  $(A_2C_4)_2$ -Ag<sub>8</sub> complex. In (A), the Big Dipper arrangement of the silvers is shown with a 3 Ag handle and a 5 Ag dipper (adapted from ref 16). In (B), silver atoms are represented by gray spheres. The electron density  $F_0 - F_c$  omit map for the silver atoms is displayed in green at a  $3\sigma$  cutoff. (C) Representation of the protonation states for the cytosine C4-NH<sub>2</sub> groups for the C(4)C(5)C(6) nucleobases in strands A and B. The cytosine—cytosine base pairs are propeller twisted by  $\sim$ 60°, as indicated by the curved arrows. (D) Representation of the protonation states for A(1)A(2)C(3) in strand A and A(1)\*A(2)C(3) in strand B, where A(1)\* is from a neighboring, symmetry-related strand. The neutron scattering length density  $F_0 - F_c$  is displayed in magenta at a  $3\sigma$  cutoff, and the atoms are colored as follows: carbon, green; nitrogen, blue; oxygen, red; hydrogen, white; deuterium, cyan; silver, gray.<sup>57</sup> (E) Two-dimensional view of a cytosine-Ag<sup>+</sup> base pair with a trans configuration of the N1–glycosidic bonds.

our study suggests how a network of bonds controls the spectra of these supramolecular chromophores.

 $(A_2C_4)_2$ -Ag<sub>8</sub> crystals were grown to sizes of  $\sim 0.8 \times \sim 0.5 \times 10^{-2}$ ~0.5 mm<sup>3</sup>, and diffraction was measured on the Macromolecular Neutron Diffractometer.<sup>31</sup> Within the parallel  $[A(1)A(2)C(3)C(4)C(5)C(6)]_2$  duplex, two substructures organize the 8 silvers identically in the cryogenic and room temperature X-ray diffraction studies (Figures 1A,B). We first consider the matched set of  $[C(4)C(5)C(6)]_2$  nucleobases. Opposing cytosines are cross-linked by silvers that bind to the N3 sites, which are Lewis bases that are deprotonated at neutral pH and bind silver (Figure 1C). <sup>29,32</sup> The cytosines in this duplex are arranged so that hydrogen bonds also develop between proximal functional groups. As observed with other parallel duplexes, opposing cytosines are configured with trans N1-glycosidic bonds, and the approximate mirror-image symmetry of the cytosines yields neighboring C4-NH2 and C2-O groups (Figure 1E).<sup>26</sup> Because the cytosines are twisted with respect to each other, inter- vs intrabase pair hydrogen bonds can develop (Figure 1F). On the basis of inferred hydrogen positions in the X-ray diffraction data, the measured N-H/O bond distances of 1.9-2.5 Å are consistent with hydrogen bonds.<sup>33</sup> To directly identify these hydrogens, isotope exchange with D2O was used because deuterium scatters neutrons more efficiently than hydrogen.<sup>34</sup> Neutron scattering length density (NSLD) maps show that the former exocyclic amines are fully protonated/deuterated and thus capable of hydrogen bonding (Figure 1C). The combination of both silver and hydrogen bonds supports a metal-mediated sub-duplex within the overall  $(A_2C_4)_2$ -Ag<sub>8</sub> complex.<sup>35</sup> Collective interactions of silvers and hydrogens with nucleobases have also be identified in related complexes using mass spectrometry, spectroscopic, and calorimetry/ structural studies.36,37 For example, cytosine strands form duplexes whose strands are linked via both Ag<sup>+</sup> with inter- and intranucleobase hydrogen bonds. <sup>38,39</sup> These interactions open new paths to DNA nanostructures and nanomachines.<sup>40</sup>

This sub-duplex shares key structural features with other DNA complexes with oxidized silvers:  $Ag^+$ –DNA bond lengths of 2.1-2.2 Å,  $N-Ag^+$ –N bond angles of  $164^\circ-176^\circ$ , and base pairs twisted by  $30^\circ-60^\circ.^{41-44}$  Here, we consider thermodynamic similarities by reacting  $Ag^+$  with a  $A_2C_4$  duplex and measuring the  $Ag^+$  stoichiometry and affinity using isothermal titration calorimetry. This reaction was considered because silver cluster chromophores, such as the green emitting  $Ag_{10}^{6+}$  and the near-infrared emitting  $Ag_{30}^{18+}$ , can be significantly oxidized. We consider that the  $Ag^+$  and  $Ag^0$  may be distinct components within a DNA–cluster complex. To mimic the  $(A_2C_4)_2$  duplex observed in the crystal structure, two  $A_2C_4$  strands were covalently linked via an inert triethylene glycol (see the inset in Figure 2). To match the structure in the

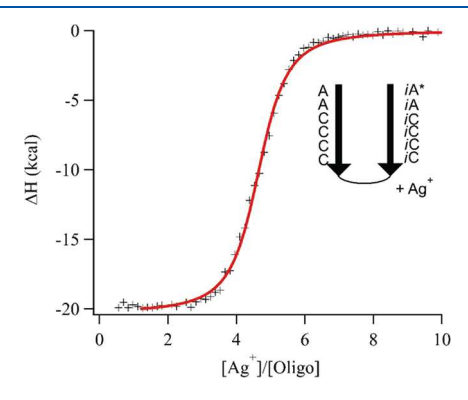


Figure 2. Binding isotherm from the titration of 1 mM  $Ag^+$  into  $5 \mu M$  of the  $(A_2C_4)_2$  dimer at 20 °C. The fit in red describes a single site model that yielded the stoichiometry, affinity, and enthalpy change. The inset shows the structure of  $(A_2C_4)$ -teg- $(iA_2iC_4)$  with the triethylene glycol represented by the loop between the  $A2C_4$ - $A_2$ - $iC_4$ T strands. This structure assumes that the symmetry-related A(1)B in the crystal structure can be replaced by  $A^*$  in this dimer. The flipped arrow and the "i" show that the polarity of these nucleobases is the reversed  $A' \to A'$  polarity.

crystal, backbone polarities were synthetically reversed, with the leading  $A_2C_4$  having the normal  $5' \rightarrow 3'$  direction and the lagging  $A_2C_4$  having the opposite  $3' \rightarrow 5'$  direction. <sup>25,49</sup> This structure assumes that  $A(1)_B^*$  is an artifact of crystallization and can be substituted with the corresponding adenine within a single dimer (see Figure 1D and insert in Figure 2). This composite strand was reacted with Ag+, and the significant exothermic heat release was used to measure the Ag+-DNA enthalpy change, stoichiometry, and affinity (Figure 2). The stoichiometry of 5.0  $\pm$  0.2 Ag<sup>+</sup>/(A<sub>2</sub>C<sub>4</sub>)<sub>2</sub> duplex is larger than the 12 nucleobases in this strand, so we propose that the duplex folds and is cross-linked by Ag<sup>+</sup> adducts, as observed in the crystal structure and in other complexes (Figure 1C).<sup>36,37</sup> The affinity of  $(5.0 \pm 0.2) \times 10^6 \,\mathrm{M(Ag^+)^{-1}}$  and  $\Delta H = -15.5 \pm 0.2 \,\mathrm{M(Ag^+)^{-1}}$ 1.3 kJ/mol Ag<sup>+</sup> are consistent with the stability of other Ag<sup>+</sup>cytosine complexes.  $^{50,51}$  The  $\Delta S = -26.4 \pm 3.3$  J/K·mol Ag<sup>+</sup> may reflect the assembly of the duplex, but other factors may contribute to this change.<sup>51</sup> Because both thermodynamic and structural parameters parallel other C-Ag+-C base pairs, we suggest that the 3 handle-like silvers in the  $[C(4)C(5)C(6)]_2$ sub-duplex are Ag+. The other 2 Ag+ may be part of the neighboring substructure of this complex.

Relative to its  $[C(4)C(5)C(6)]_2$  neighbor, the [A(1)A(2)-C(3)<sub>2</sub> substructure in  $(A_2C_4)_2$ -Ag<sub>8</sub> has a distinct protonation pattern. These nucleobases chelate a trapezoidal set of five silvers, whose 2.9 Å silver bond distances support a metal-like cluster with loosely held valence electrons. This binding pocket is framed by two heteroatoms in each nucleobase: the N1 and C6-NH<sub>2</sub> from the adenines and the N3 and C4-NH<sub>2</sub> from the cytosines. The 2.1 Å nitrogen-silver bond lengths match those observed with other DNA-silver complexes, thus supporting a stable complex. 52,53 These coordination sites can also bind H<sup>+</sup>, which in this environment are not supporting but competing. The adenine N1 and cytosine N3 should be deprotonated at neutral pH because of their respective p $K_a$  values of ~3.9 and  $\sim$ 4.6; thus, these sites will be open Lewis bases for silvers. In contrast, the exocyclic C6-NH2 of adenine and the C4-NH2 of cytosine are expected to be poor Lewis bases for two reasons.<sup>54</sup> First, their lone pairs are delocalized into the aromatic nucleobases, as these amines are sp<sup>2</sup> hybridized with short, double-bond C-N bond lengths and planar NH2 geometries. 55,56 Second, these groups are expected to be fully protonated at neutral pH because their p $K_a \sim 18^{.57,58}$  Despite these impediments, X-ray diffraction shows that the silvers are anchored at these sites (Figure 1D). Most importantly, NSLD maps suggest that the C6-NH2 and C4-NH2 coordinate silvers because they are singly deprotonated (see Table 1 and the Supporting Information).

Table 1. Protonation States of A(1), A(2), and C(3) Sites in the  $(A_2C_4)$ -Ag<sub>8</sub> Complex

	protonation state
strand A	
	singly deprotonated
	singly deprotonated
	doubly protonated
strand B	
	doubly protonated
	singly deprotonated
	singly deprotonated

These exocyclic amines may be deprotonated because their nucleobases are electronically perturbed. For example, protonating or alkylating the N1 in adenine and the N3 and cytosine drops the  $pK_a$  of the ortho exocyclic amines by from ~18 to ~9, a 10<sup>8</sup> acidification. <sup>59</sup> Transition metals also acidify amines, and platinum has received the most attention because it is a cancer therapeutic. Platinum complexes with the N1 of adenine and the N3 of cytosine lower the  $pK_a$  of their respective exocyclic amines by 4-5 units. 60,61 Ruthenium complexes produce  $pK_a \sim 8$  for the C6-NH<sub>2</sub> in adenine, thus approaching the pH of neutral solutions. 62 A number of factors control this shift in acidity, such as the metal and its charge, the site of coordination in the nucleobases, and neighboring nucleobases that stabilize the conjugate base. 60,63 We consider how silver might perturb the adenine/cytosine charge distributions. Neutral silver atoms bind weakly with DNA with little charge redistribution, so we suggest that Ag<sup>+</sup> adducts could acidify the C6-NH<sub>2</sub> and C4-NH<sub>2</sub> groups.<sup>32</sup> Our calorimetry studies suggest that 5 of the 8 silvers in  $(A_2C_4)_2$ -Ag<sub>8</sub> may be Ag<sup>+</sup>, consistent with other oxidized clusters such as Ag<sub>6</sub><sup>4+</sup>, Ag<sub>10</sub><sup>6+</sup>, Ag<sub>17</sub><sup>9+</sup>, and Ag<sub>30</sub><sup>18+</sup>.  $^{26,45-47}$  Thus, we expect Ag<sup>+</sup> in a partially oxidized Ag<sub>8</sub> cluster could acidify the adenines and cytosines.

Our studies focused on protonation states of nucleotides because  $\mathrm{H}^+$  controls DNA–silver cluster fluorescence. For example, acidic solutions protonate  $\mathrm{dC_{12}}$  and quench red emission from the conjugated cluster, while basic solutions deprotonate thymine oligonucleotides to turn on green emitting clusters. Nucleobases are also protonated when they pair with their canonical partner, and the resulting DNA duplex boosts emission by changing the cluster shape. Nutleobases are reversible, suggesting that protons and silvers competitively bind to the same heteroatoms. These studies suggest that DNA is plastic ligand that is changed by its silver cluster adduct. Understanding these bonding interactions may help us better understand the spectra of these supramolecular chromophores.

In conclusion, neutron and X-ray diffraction identifies the hydrogens/deuteriums in the  $(A_2C_4)_2\text{-}Ag_8$  complex and reveals both cooperative and competitive bonds with hydrogen ions. Interbase hydrogen bonds within the C(4)C(5)C(6) subduplex cooperatively form around and may reinforce the silver—cytosine contacts. Exocyclic amines in the A(1)A(2)-C(3) region are deprotonated, and the open binding sites suggest that ancillary silvers acidify this site. These studies suggest that  $H^+$  and pH can be a tool that exogenously tunes the binding sites of DNA-bound silver clusters.

#### ASSOCIATED CONTENT

### **Supporting Information**

The Supporting Information is available free of charge at https://pubs.acs.org/doi/10.1021/acs.jpclett.2c03161.

Experimental details for crystal growth, neutron diffraction, and isothermal titration calorimetry (PDF)

Transparent Peer Review report available (PDF)

#### AUTHOR INFORMATION

#### **Corresponding Authors**

Jeffrey T. Petty – Department of Chemistry, Furman University, Greenville, South Carolina 29613, United States; orcid.org/0000-0003-0149-5335; Email: jpetty@furman.edu

Flora Meilleur — Department of Molecular and Structural Biochemistry, North Carolina State University, Raleigh, North Carolina 27695, United States; Neutron Scattering Division, Oak Ridge National Laboratory, Oak Ridge, Tennessee 37831, United States; orcid.org/0000-0001-9313-8989; Email: meilleurf@ornl.gov

#### Authors

Fred David – Department of Chemistry, Furman University, Greenville, South Carolina 29613, United States

Caleb Setzler – Department of Chemistry, Furman University, Greenville, South Carolina 29613, United States

Alexandra Sorescu – Department of Chemistry, Furman University, Greenville, South Carolina 29613, United States

Raquel L. Lieberman — School of Chemistry & Biochemistry, Georgia Institute of Technology, Atlanta, Georgia 30332-0400, United States; orcid.org/0000-0001-9345-3735

Complete contact information is available at: https://pubs.acs.org/10.1021/acs.jpclett.2c03161

#### Notes

The authors declare no competing financial interest.

### ■ ACKNOWLEDGMENTS

We thank the National Science Foundation (CHE-1611451 and CHE-2002910) and the Furman Advantage program. This work was supported in part by the National Science Foundation EPSCoR Program under NSF Award OIA-1655740. Any opinions, findings and conclusions or recommendations expressed in this material are those of the author(s) and do not necessarily reflect those of the National Science Foundation. A portion of this research used resources at the High Flux Isotope Reactor and Spallation Neutron Source, DOE Office of Science User Facilities operated by the Oak Ridge National Laboratory.

#### REFERENCES

- (1) Gwinn, E.; Schultz, D.; Copp, S.; Swasey, S. DNA-protected silver clusters for nanophotonics. *Nanomaterials* **2015**, *5*, 180–207.
- (2) Gonzàlez-Rosell, A.; Cerretani, C.; Mastracco, P.; Vosch, T.; Copp, S. M. Structure and luminescence of DNA-templated silver clusters. *Nanoscale Advances* **2021**, *3*, 1230–1260.
- (3) Petty, J. T.; Zheng, J.; Hud, N. V.; Dickson, R. M. DNA-templated ag nanocluster formation. *J. Am. Chem. Soc.* **2004**, *126*, 5207–12.
- (4) Vosch, T.; Antoku, Y.; Hsiang, J.-C.; Richards, C. I.; Gonzalez, J. I.; Dickson, R. M. Strongly emissive individual DNA-encapsulated Ag nanoclusters as single-molecule fluorophores. *Proc. Natl. Acad. Sci. U. S. A.* 2007, 104, 12616–12621.
- (5) Schultz, D.; Gardner, K.; Oemrawsingh, S. S. R.; Markeševic', N.; Olsson, K.; Debord, M.; Bouwmeester, D.; Gwinn, E. Evidence for rod-shaped DNA-stabilized silver nanocluster emitters. *Adv. Mater.* **2013**, *25*, 2797–2803.
- (6) Zhao, T.-T.; Chen, Q.-Y.; Zeng, C.; Lan, Y.-Q.; Cai, J.-G.; Liu, J.; Gao, J. Multi-DNA-Ag nanoclusters: Reassembly mechanism and sensing the change of hif in cells. *J. Mater. Chem. B* **2013**, *1*, 4678–4683.
- (7) Song, C.; Xu, J.; Chen, Y.; Zhang, L.; Lu, Y.; Qing, Z. DNA-templated fluorescent nanoclusters for metal ions detection. *Molecules* **2019**, *24*, 4189.
- (8) Richards, C. I.; Choi, S.; Hsiang, J.-C.; Antoku, Y.; Vosch, T.; Bongiorno, A.; Tzeng, Y.-L.; Dickson, R. M. Oligonucleotide-

- stabilized Ag nanocluster fluorophores. J. Am. Chem. Soc. 2008, 130, 5038-5039.
- (9) Copp, S. M.; Bogdanov, P.; Debord, M.; Singh, A.; Gwinn, E. Base motif recognition and design of DNA templates for fluorescent silver clusters by machine learning. *Adv. Mater.* **2014**, *26*, 5839–5845.
- (10) Yeh, H. C.; Sharma, J.; Han, J. J.; Martinez, J. S.; Werner, J. H. A DNA-silver nanocluster probe that fluoresces upon hybridization. *Nano Lett.* **2010**, *10*, 3106–10.
- (11) Petty, J. T.; Giri, B.; Miller, I. C.; Nicholson, D. A.; Sergev, O. O.; Banks, T. M.; Story, S. P. Silver clusters as both chromophoric reporters and DNA ligands. *Anal. Chem.* **2013**, *85*, 2183–2190.
- (12) Sharma, J.; Yeh, H. C.; Yoo, H.; Werner, J. H.; Martinez, J. S. Silver nanocluster aptamers: In situ generation of intrinsically fluorescent recognition ligands for protein detection. *Chem. Commun.* **2011**, *47*, 2294–2296.
- (13) Lin, X.; Zou, L.; Lan, W.; Liang, C.; Yin, Y.; Liang, J.; Zhou, Y.; Wang, J. Progress of metal nanoclusters in nucleic acid detection. *Dalton Trans.* **2021**, *51*, 27–39.
- (14) Obliosca, J. M.; Liu, C.; Batson, R. A.; Babin, M. C.; Werner, J. H.; Yeh, H.-C. DNA/rna detection using DNA-templated few-atom silver nanoclusters. *Biosensors* **2013**, *3*, 185–200.
- (15) Khatun, E.; Bodiuzzaman, M.; Sugi, K. S.; Chakraborty, P.; Paramasivam, G.; Dar, W. A.; Ahuja, T.; Antharjanam, S.; Pradeep, T. Confining an  $Ag_{10}$  core in an  $Ag_{12}$  shell: A four-electron superatom with enhanced photoluminescence upon crystallization. *ACS Nano* **2019**, *13*, 5753–5759.
- (16) Zhang, S.-S.; Havenridge, S.; Zhang, C.; Wang, Z.; Feng, L.; Gao, Z.-Y.; Aikens, C. M.; Tung, C.-H.; Sun, D. Sulfide boosting near-unity photoluminescence quantum yield of silver nanocluster. *J. Am. Chem. Soc.* **2022**, *144*, 18305–18314.
- (17) Wang, Z.; Li, L.; Feng, L.; Gao, Z.-Y.; Tung, C.-H.; Zheng, L.-S.; Sun, D. Solvent-controlled condensation of  $[Mo_2O_5(PtC_4A)_2]_6^-$  metalloligand in stepwise assembly of hexagonal and rectangular  $Ag_{18}$  nanoclusters. *Angew. Chem., Int. Ed. Engl.* **2022**, *61*, e202200823.
- (18) Cerretani, C.; Kanazawa, H.; Vosch, T.; Kondo, J. Crystal structure of a nir-emitting DNA-stabilized ag<sub>16</sub> nanocluster. *Angew. Chem., Int. Ed. Engl.* **2019**, *58*, 17153–17157.
- (19) Huard, D. J. E.; Demissie, A.; Kim, D.; Lewis, D.; Dickson, R. M.; Petty, J. T.; Lieberman, R. L. Atomic structure of a fluorescent Ag<sub>8</sub> cluster templated by a multistranded DNA scaffold. *J. Am. Chem. Soc.* **2019**, *141*, 11465–11470.
- (20) Cerretani, C.; Kondo, J.; Vosch, T. Mutation of position 5 as a crystal engineering tool for a nir-emitting DNA-stabilized Ag16 nanocluster. *CrystEngComm.* **2020**, 22, 8136–8141.
- (21) Desireddy, A.; Conn, B. E.; Guo, J.; Yoon, B.; Barnett, R. N.; Monahan, B. M.; Kirschbaum, K.; Griffith, W. P.; Whetten, R. L.; Landman, U.; Bigioni, T. P. Ultrastable silver nanoparticles. *Nature* **2013**, *501*, 399–402.
- (22) Yang, H.; Wang, Y.; Huang, H.; Gell, L.; Lehtovaara, L.; Malola, S.; Häkkinen, H.; Zheng, N. All-thiol-stabilized  $Ag_{44}$  and  $Au_{12}Ag_{32}$  nanoparticles with single-crystal structures. *Nat. Commun.* **2013**, *4*, 2422–2429.
- (23) Zheng, J.; Nicovich, P. R.; Dickson, R. M. Highly fluorescent noble-metal quantum dots. *Annu. Rev. Phys. Chem.* **2007**, *58*, 409–431.
- (24) Henglein, A.; Mulvaney, P.; Linnert, T. Chemistry of agn aggregates in aqueous-solution nonmetallic oligomeric clusters and metallic particles. *Faraday Discuss.* **1991**, *92*, 31–44.
- (25) Petty, J. T.; Lewis, D.; Carnahan, S.; Kim, D.; Couch, C. Tugof-war between DNA chelation and silver agglomeration in DNA-silver cluster chromophores. *J. Phys. Chem. B* **2022**, *126*, 3822–3830.
- (26) Petty, J. T.; Sergev, O. O.; Ganguly, M.; Rankine, I. J.; Chevrier, D. M.; Zhang, P. A segregated, partially oxidized, and compact Ag<sub>10</sub> cluster within an encapsulating DNA host. *J. Am. Chem. Soc.* **2016**, 138, 3469–3477.
- (27) Copp, S. M.; Schultz, D.; Swasey, S.; Pavlovich, J.; Debord, M.; Chiu, A.; Olsson, K.; Gwinn, E. Magic numbers in DNA-stabilized fluorescent silver clusters lead to magic colors. *J. Phys. Chem. Lett.* **2014**, *5*, 959–963.

- (28) Müller, J. Nucleic acid duplexes with metal-mediated base pairs and their structures. *Coord. Chem. Rev.* **2019**, 393, 37–47.
- (29) Ritchie, C. M.; Johnsen, K. R.; Kiser, J. R.; Antoku, Y.; Dickson, R. M.; Petty, J. T. Ag nanocluster formation using a cytosine oligonucleotide template. *J. Phys. Chem. C* **2007**, *111*, 175–181.
- (30) Sengupta, B.; Ritchie, C. M.; Buckman, J. G.; Johnsen, K. R.; Goodwin, P. M.; Petty, J. T. Base-directed formation of fluorescent silver clusters. *J. Phys. Chem. C* **2008**, *112*, 18776–18782.
- (31) Meilleur, F.; Coates, L.; Cuneo, M. J.; Kovalevsky, A.; Myles, D. A. A. The neutron macromolecular crystallography instruments at Oak Ridge National Laboratory: Advances, challenges, and opportunities. *Crystals* **2018**, *8*, 388.
- (32) Soto-Verdugo, V.; Metiu, H.; Gwinn, E. The properties of small Ag clusters bound to DNA bases. *J. Chem. Phys.* **2010**, *132*, 195102.
- (33) Szalewicz, K. Hydrogen bond. In *Encyclopedia of Physical Science and Technology*, 3rd ed.; Meyers, R. A., Ed.; Academic Press: New York, 2003; pp 505–538.
- (34) Schroder, G. C.; Meilleur, F. Neutron crystallography data collection and processing for modelling hydrogen atoms in protein structures. *J. Vis. Exp.* **2020**, *166*, 1–38.
- (35) Lippert, B. Metal-modified base pairs" vs. "Metal-mediated pairs of bases": Not just a semantic issue! *JBIC Journal of Biological Inorganic Chemistry* **2022**, 27, 215–219.
- (36) Swasey, S. M.; Leal, L. E.; Lopez-Acevedo, O.; Pavlovich, J.; Gwinn, E. G. Silver (I) as DNA glue: Ag<sup>+</sup>-mediated guanine pairing revealed by removing Watson-Crick constraints. *Sci. Rep.* **2015**, *5*, 10163–10170.
- (37) Loo, K.; Degtyareva, N.; Park, J.; Sengupta, B.; Reddish, M.; Rogers, C. C.; Bryant, A.; Petty, J. T. Ag<sup>+</sup>-mediated assembly of 5′-guanosine monophosphate. *J. Phys. Chem. B* **2010**, *114*, 4320–4326.
- (38) Chen, X.; Karpenko, A.; Lopez-Acevedo, O. Silver-mediated double helix: Structural parameters for a robust DNA building block. *ACS Omega* **2017**, *2*, 7343–7348.
- (39) Swasey, S. M.; Rosu, F.; Copp, S. M.; Gabelica, V.; Gwinn, E. G. Parallel guanine duplex and cytosine duplex DNA with uninterrupted spines of Ag-I-mediated base pairs. *J. Phys. Chem. Lett.* **2018**, *9*, 6605–6610.
- (40) Jash, B.; Müller, J. Metal-mediated base pairs: From characterization to application. *Chem.—Eur. J.* **2017**, 23, 17166–17178.
- (41) Clever, G. H.; Kaul, C.; Carell, T. DNA-metal base pairs. *Angew. Chem., Int. Ed. Engl.* **2007**, *46*, 6226–6236.
- (42) Kondo, J.; Tada, Y.; Dairaku, T.; Hattori, Y.; Saneyoshi, H.; Ono, A.; Tanaka, Y. A metallo-DNA nanowire with uninterrupted one-dimensional silver array. *Nat. Chem.* **2017**, *9*, 956–960.
- (43) Terron, A.; Tomas, L.; Bauza, A.; Garcia-Raso, A.; Fiol, J. J.; Molins, E.; Frontera, A. The first x-ray structure of a silver-nucleotide complex: Interaction of ion Ag(I) with cytidine-5 '-monophosphate. *CrystEngComm.* **2017**, *19*, 5830–5834.
- (44) Mistry, L.; Waddell, P. G.; Wright, N. G.; Horrocks, B. R.; Houlton, A. Transoid and cisoid conformations in silver-mediated cytosine base pairs: Hydrogen bonding dictates argentophilic interactions in the solid state. *Inorg. Chem.* **2019**, *58*, 13346–13352.
- (45) Swasey, S. M.; Copp, S. M.; Nicholson, H. C.; Gorovits, A.; Bogdanov, P.; Gwinn, E. G. High throughput near infrared screening discovers DNA-templated silver clusters with peak fluorescence beyond 950 nm. *Nanoscale* **2018**, *10*, 19701–19705.
- (46) Gonzàlez-Rosell, A.; Guha, R.; Cerretani, C.; Rück, V.; Liisberg, M. B.; Katz, B. B.; Vosch, T.; Copp, S. M. DNA stabilizes eight-electron superatom silver nanoclusters with broadband down-conversion and microsecond-lived luminescence. *J. Phys. Chem. Lett.* **2022**, *13*, 8305–8311.
- (47) Koszinowski, K.; Ballweg, K. A highly charged Ag<sub>6</sub><sup>4+</sup> core in a DNA-encapsulated silver nanocluster. *Chem.—Eur. J.* **2010**, *16*, 3285–3290.
- (48) Petty, J. T.; Ganguly, M.; Rankine, I. J.; Baucum, E. J.; Gillan, M. J.; Eddy, L. E.; Léon, J. C.; Müller, J. Repeated and folded DNA sequences and their modular  $Ag_{10}^{6+}$  cluster. *J. Phys. Chem. C* **2018**, 122, 4670–4680.

- (49) van de Sande, J. H.; Ramsing, N. B.; Germann, M. W.; Elhorst, W.; Kalisch, B. W.; Kitzing, E. v.; Pon, R. T.; Clegg, R. C.; Jovin, T. M. Parallel stranded DNA. *Science* **1988**, 241, 551–557.
- (50) Torigoe, H.; Miyakawa, Y.; Ono, A.; Kozasa, T. Thermodynamic properties of the specific binding between Ag+ ions and C:C mismatched base pairs in duplex DNA. *Nucleosides, Nucleotides & Nucleic Acids* **2011**, *30*, 149–167.
- (51) Torigoe, H.; Okamoto, I.; Dairaku, T.; Tanaka, Y.; Ono, A.; Kozasa, T. Thermodynamic and structural properties of the specific binding between Ag<sup>+</sup> ion and C:C mismatched base pair in duplex DNA to form C–Ag–C metal-mediated base pair. *Biochimie* **2012**, *94*, 2431–2440.
- (52) Kistenmacher, T. J.; Rossi, M.; Marzilli, L. G. Crystal and molecular structure of (nitrato)(1-methylcytosine)silver(I): An unusual crosslinked polymer containing a heavy metal and a modified nucleic acid constituent. *Inorg. Chem.* 1979, 18, 240–244.
- (53) Menzer, S.; Sabat, M.; Lippert, B. Ag(i) modified base-pairs involving complementary (G,C) and noncomplementary (A,C) nucleobases on the possible structural role of aqua ligands in metal-modified nucleobase pairs. *J. Am. Chem. Soc.* **1992**, *114*, 4644–4649.
- (54) Lippert, B.; Sanz Miguel, P. J. The renaissance of metal—pyrimidine nucleobase coordination chemistry. *Acc. Chem. Res.* **2016**, 49, 1537–1545.
- (55) Shoup, R. R.; Miles, H. T.; Becker, E. D. Restricted rotation about the exocyclic carbon-nitrogen bond in cytosine derivatives. *J. Phys. Chem.* **1972**, *76*, 64–70.
- (56) Silaghi-Dumitrescu, R.; Mihály, B.; Mihály, T.; Attia, A. A. A.; Sanz Miguel, P. J.; Lippert, B. The exocyclic amino group of adenine in Pt(II) and Pd(II) complexes: A critical comparison of the x-ray crystallographic structural data and gas phase calculations. *J. Biol. Inorg. Chem.* **2017**, *22*, 567–579.
- (57) Harris, M. G.; Stewart, R. Amino group acidity in amino-pyridines and aminopyrimidines. *Can. J. Chem.* 1977, 55, 3800–3806.
- (58) Bloomfield, V. A.; Crothers, D. M.; Tinoco, I., Jr. Nucleic acids: Structures, Properties, and Functions; University Science Books: Sausaltio, CA, 2000; p 794; Chapter 14.
- (59) Kettani, A.; Guéron, M.; Leroy, J. L. Amino proton exchange processes in mononucleosides. *J. Am. Chem. Soc.* **1997**, *119*, 1108–1115.
- (60) Garijo Añorbe, M.; Lüth, M. S.; Roitzsch, M.; Morell Cerdà, M.; Lax, P.; Kampf, G.; Sigel, H.; Lippert, B. Perturbation of the NH $_2$  pKa value of adenine in platinum(II) complexes: Distinct stereochemical internucleobase effects. *Chem.—Eur. J.* **2004**, *10*, 1046–1057
- (61) Lippert, B. Alterations of nucleobase pK<sub>a</sub> values upon metal coordination: Origins and consequences. *Prog. Inorg. Chem.* **2005**.
- (62) Clarke, M. J. Ruthenium in biology: DNA interactions. In *Electron Transfer Reactions*; American Chemical Society: 1997; Vol. 253, pp 349–365.
- (63) Pesch, F. J.; Preut, H.; Lippert, B. Mixed nucleobase, amino acid complexes of pt(ii). Preparation and x-ray structure of trans-[(CH<sub>3</sub>NH<sub>2</sub>)<sub>2</sub>Pt(1-MeC-N<sub>3</sub>)(Gly-N)]NO<sub>3</sub>·2H<sub>2</sub>O and its precursor trans-[(CH<sub>3</sub>NH<sub>2</sub>)<sub>2</sub>Pt(1-MeC-N<sub>3</sub>)Cl]Cl·H<sub>2</sub>O. *Inorg. Chim. Acta* **1990**, *169*, 195–200.
- (64) Yang, S. W.; Vosch, T. Rapid detection of microRNA by a silver nanocluster DNA probe. *Anal. Chem.* **2011**, *83*, 6935–6939.
- (65) Petty, J. T.; Ganguly, M.; Rankine, I. J.; Chevrier, D. M.; Zhang, P. A DNA-encapsulated and fluorescent  $Ag_{10}^{6+}$  cluster with a distinct metal-like core. *J. Phys. Chem. C* **2017**, *121*, 14936–14945.
- (66) Blevins, M. S.; Kim, D.; Crittenden, C. M.; Hong, S.; Yeh, H.-C.; Petty, J. T.; Brodbelt, J. S. Footprints of nanoscale DNA–silver cluster chromophores via activated-electron photodetachment mass spectrometry. ACS Nano 2019, 13, 14070–14079.
- (67) Ganguly, M.; Bradsher, C.; Goodwin, P.; Petty, J. T. DNA-directed fluorescence switching of silver clusters. *J. Phys. Chem. C* **2015**, *119*, 27829–27837.

(68) Petty, J. T.; Sergev, O. O.; Nicholson, D. A.; Goodwin, P. M.; Giri, B.; McMullan, D. R. A silver cluster—DNA equilibrium. *Anal. Chem.* **2013**, *85*, 9868—9876.

# **TRECOMMENDED** Recommended by ACS

DNA Stabilizes Eight-Electron Superatom Silver Nanoclusters with Broadband Downconversion and Microsecond-Lived Luminescence

Anna Gonzàlez-Rosell, Stacy M. Copp, et al.

AUGUST 29, 2022

THE JOURNAL OF PHYSICAL CHEMISTRY LETTERS

READ 🗹

Chemistry-Informed Machine Learning Enables Discovery of DNA-Stabilized Silver Nanoclusters with Near-Infrared Fluorescence

Peter Mastracco, Stacy M. Copp, et al.

SEPTEMBER 20, 2022

ACS NANO

READ **C** 

Predicting the Fluorescence Properties of Hairpin-DNA-Templated Silver Nanoclusters via Deep Learning

Fuheng Zhai, Ronghuan He, et al.

JULY 05, 2022

ACS APPLIED NANO MATERIALS

READ 🗹

A Reciprocal-Amplifiable Fluorescence Sensing Platform via Replicated Hybridization Chain Reaction for Hosting Concatenated Multi-Ag Nanoclusters as Signal Reporter

Mengdie Li, Wenju Xu, et al.

NOVEMBER 15, 2022

ANALYTICAL CHEMISTRY

READ 🗹

Get More Suggestions >

Mapping H<sup>+</sup> in the Nanoscale (A<sub>2</sub>C<sub>4</sub>)<sub>2</sub>-Ag<sub>8</sub> Fluorophore

Fred David<sup>†</sup>, Caleb Setzler<sup>†</sup>, Alexandra Sorescu<sup>†</sup>, Raquel L. Lieberman<sup>‡</sup>, Flora Meilleur<sup>§</sup>\*, and

Jeffrey T. Petty\*\*

<sup>†</sup>Department of Chemistry, Furman University, Greenville, SC 29613, USA

<sup>‡</sup>School of Chemistry & Biochemistry Georgia Institute of Technology Atlanta GA 30332-0400,

USA

§Department of Molecular and Structural Biochemistry, North Carolina State University,

Campus Box 7622, Raleigh, NC 27695, USA

and

Neutron Scattering Division, Oak Ridge National Laboratory, PO Box 2008, Oak Ridge, TN 37831, USA.

## **Experimental Methods:** Crystal Growth

An ~1.5 µmole sample of desalted AACCCC (Integrated DNA Technologies) was diluted to 15 mL with water and then concentrated to ~5 mM using dialysis at 8 °C (Vivaspin 15R, 2000 MWCO). Crystals were grown using sitting drop vapor diffusion. The drops with a volume of 40 μL containing 0.9 mM A<sub>2</sub>C<sub>4</sub>, 6.5 equivalents of AgNO<sub>3</sub>, and 375 mM cacodylate buffer at pH = 6.5 were equilibrated against a 750-µL reservoir composed of 34 or 36 % MPD. The crystals grew at 29 °C to sizes of  $\sim 0.8 \text{ x} \sim 0.5 \text{ x} \sim 0.5 \text{ mm}$  in  $\sim 2 \text{ days}$ . Crystals were mounted in capillaries for room temperature data collection as described by Schröder and Meilleur.<sup>17</sup> Quartz capillaries (1.0 mm id, 1.2 mm od, VitroCom), shortened to a length of  $\sim$ 5 cm, were loaded with  $\sim$ 10  $\mu$ L of the crystallization buffer at one end. Crystals were harvested using a microloop and transferred to the crystallization solution in the quartz capillaries. Gravity was used to position the crystal in the middle of the capillary. The hydrogenated solution was then dried out using absorbent paper. Plugs of crystallization buffer prepared in D<sub>2</sub>O (99.9% D, Cambridge Isotopes) were inserted into both ends of the capillary. The capillary ends were then sealed with beeswax. The crystals were left to equilibrate for more than two months to exchange the hydrogen to deuterium via vapor exchange prior to neutron data collection. High D<sub>2</sub>O purity and extended vapor exchange period are important to achieve high H/D exchange level.

### Neutron and X-ray crystallographic data collection and structure refinement

Initial white beam neutron diffraction tests were performed on the IMAGINE beamline at the High Flux Isotope Reactor (HFIR). Neutron time-of-flight diffraction data were collected at room temperature on the MaNDi instrument at the Spallation Neutron Source (SNS). An incident neutron wavelength range of 2 Å to 4 Å was used. A total of 9 diffraction images were collected with a  $\Delta \phi$  of 10° between frames and an average exposure of 24 hours per image. The neutron diffraction data extended to a resolution of 2.1 Å. Following neutron diffraction data collection, an X-ray dataset was collected on the same crystal at room temperature on a microfocus rotating anode X-ray diffractometer. The X-ray diffraction data extended to a resolution of 1.8 Å.

The neutron dataset was reduced using the *Mantid* package<sup>23</sup> and integrated using three dimensional profile fitting.<sup>24</sup> The data were wavelength normalized using *LAUENORM* from the *LAUEGEN* suite<sup>25-27</sup> and further scaled using SCALA from the CCP4 suite.<sup>28-29</sup> The X-ray data were indexed, integrated using *CrysAlis PRO* (Rigaku, Woodlands, Texas, USA) and scaled and merged with *AIMLESS* in the *CCP4* suite.<sup>30</sup> The data reduction statics are presented in Table 1. We use an "X-ray then Neutron" refinement strategy whereby a model was first refined against the X-ray data alone prior to refining a second model, including hydrogen/deuterium atoms, against the neutron data alone. This strategy is preferred for complex containing metal centers

because they are prone to X-ray induced photoreduction and we previously observed photoreduction. In contrast, neutron radiation do not perturb metal scenters. In contrast, neutron radiation do not perturb metal scenters. In contrast, neutron radiation do not perturb metal scenters. In contrast, neutron radiation do not perturb metal scenters. In contrast, neutron radiation do not perturb metal scenters. In contrast, neutron radiation do not perturb metal scenters. In contrast, neutron data. Positional Ag atoms were do not perturb metal scenters. In contrast, neutron data phenix refine in the Phenix suite. Water molecules and Ag atoms were built manually in Coot. Hydrogen and deuterium atoms were added to the final room temperature model using phenix.ready\_set at nonexchangeable and exchangeable positions, respectively. This model was used to phase the neutron data. Positional, B-factor and occupancy refinements were performed using phenix.refine.

Initially, we added deuterium and hydrogen atoms to the model refined against the X-ray data using phenix.ready set. Phenix.ready set uses the program REDUCE (Word, et al.(1999). J. Mol. Biol. 285, 1735-1747) to add hydrogen/deuterium atoms in standardized geometry. The model generated contained H and D atoms in 0.5:0.5 ratio and was refined against the neutron data. The NSLD maps and the refined H:D exchange ratios were then inspected. This approach led to two types of H/D sites: type 1) H/D atom pointing away from the Ag atoms with these positions having high D occupancy; and type 2) H/D atoms positioned between the exocyclic N6 or N4 and the Ag atoms with refined H:D ratio of ~0.65:0.35. While this later ratio is experimentally possible, it most often signals an absence of H/D atoms at the concerned position (i.e. deprotonation) because the scattering length of H (-3.74 fm) and the scattering length of D (+6.67 fm) cancel each other at that specific ratio. To avoid the uncertainty arising from H:D ratios in the model, we then generated only deuterium atoms at all the exchangeable position. Neutron scattering length density (NSLD) Polder maps were calculated for all exocyclic amino groups to determine the protonation state of the nitrogen atoms.<sup>34</sup> The nuclear density supported modeling of deuterium atoms with 100% occupancy at all the predicted position (Fig. 1) except for the exocyclic group of A(2) from strand B which was best modeled as 75%H/25%D. As discussed above, this ratio does not allow us to fully rule out that the C6-NH<sub>2</sub> A(2) from strand B is doubly deprotonated. However, there is no chemical rational to explain a fully deprotonated C6-NH<sub>2</sub> and therefore we conclude that exchange is limited at this site and that this N is singly deprotonated. Using this approach, no residual nuclear density was left, indicating that there was no deuterium between the N6 or N4 and the Ag atoms. In the crystal structure presented here, we observed the exocyclic amine group of A(1) of strand B to be singly deprotonated. This protonation state is likely due to the crystal packing which positions an Ag atom between this group and the N1 atom of a A(1) of symmetry related molecule. Refinement statistics for the Xray and neutron models are shown in Table S1. The neutron model was deposited in the Protein Data Bank (ID: 8DYK).

Table S1. Data collection and refinement statistics.

	X-ray	Neutron
Data collection	v	
Wavelength (Å)	1.54	2-4
Resolution range (Å)	16.78 - 1.8 (1.864 - 1.8)	11.67 - 2.1 (2.175 - 2.1)
Space group	P 41 21 2	P 41 21 2
Unit cell		
a, b, c (Å)	33.57, 33.57, 63.74	33.57, 33.57, 63.74
α, β, γ (°)	90, 90, 90	90, 90, 90
Total reflections	39596 (2755)	14260 (1216)
Unique reflections	3715 (362)	2308 (216)
Multiplicity	10.7 (7.6)	6.2 (5.6)
Completeness (%)	99.4 (98.1)	96.5 (95.2)
Mean I/sigma(I)	27.9 (7.5)	10.5 (3.8)
Wilson B-factor (Å <sup>2</sup> )	12.8	13.1
R-merge	0.133 (0.345)	0.146 (0.264)
R-meas	0.140 (0.373)	0.159 (0.290)
R-pim	0.042 (0.135)	0.060 (0.115)
CĈ1/2	0.974 (0.880)	0.991 (0.328)
CC*	0.993 (0.968)	0.998 (0.703)
Refinement and model quality		,
Reflections used in refinement	3705 (358)	2307 (216)
Reflections used for R-free	371 (36)	232 (20)
R-work	0.093 (0.127)	0.229 (0.295)
R-free	0.109 (0.143)	0.288 (0.330)
CC (work)	0.972 (0.949)	0.959 (0.464)
CC (free)	0.983 (0.833)	0.870 (0.486)
Number of non-hydrogen atoms	262	265
Number of hydrogen/Deuterium	0	166
atoms		
Ligands	Ag: 12	Ag: 12
Water molecules	O: 20	O: 6
		DOD: 18
R.M.S.D. bonds (Å)	0.019	0.084
R.M.S.D. angles (°)	2.15	0.80
Clashscore	8.00	7.96

Average B-factor (Å <sup>2</sup> )			
Macromolecules	18.21	18.74	
Ligands	14.81	10.92	
Solvent	23.34	22.12	

Statistics for the highest-resolution shell are shown in parentheses.

# **Calorimetry**

Calorimetry studies used the covalently linked dimer (AACCCC)-teg-(iAiAiCiCiCiC) in which two  $A_2C_4$  strands were linked via a triethylene glycol (teg). The two  $A_2C_4$  strands are distinguished by the polarities of their phosphodiester backbones, which run  $5^{\circ} \rightarrow 3^{\circ}$  for C1-A6 and switches to  $3^{\circ} \rightarrow 5^{\circ}$  for iC7-iC10 using a  $3^{\circ}$ - $3^{\circ}$  internucleotide linkage, where the nucleobase numbers represent their positions in the strand. The teg linker does not bind silvers and does not disrupt the cluster binding site. Calorimetry studies were conducted using a Microcal VP-ITC instrument (Northhampton, MA) controlled by the Origin 7.0 software. Following degassing, a solution of AgNO<sub>3</sub> was titrated into a 5  $\mu$ M oligonucleotide solution. Heat changes associated with the titration were determined by integrating the power required to maintain reference and sample cells at the same temperature. Heat changes associated with dilution of Ag+were subtracted after saturation of the binding sites. The single site binding model in the manufacturer software was appropriate for fitting the binding isotherms to determine the enthalpy and free energy changes and the adduct stoichiometry. Entropy changes were derived from the free energy and enthalpy changes. Uncertainties were derived from three experiments on separate samples.

#### jz-2022-03161k.R1

Name: Peer Review Information for "Mapping H<sup>+</sup> in the Nanoscale (A<sub>2</sub>C<sub>4</sub>)<sub>2</sub>-Ag<sub>8</sub> Fluorophore"

First Round of Reviewer Comments

#### Reviewer: 1

#### Comments to the Author

The authors propose to determine the hydrogen/deuterium in the DNA-bound silver clusters: (A2C4)2-Ag8 complex via neutron and X-ray diffraction, revealing cooperative and competitive bonding with the hydrogen ions. Besides, the DNA host has two substructures with fully protonated and deprotonated patterns, which perturb the electron distribution in the aromatic nucleobases, further tune the electronic spectra of such complex. The study is interesting and solid, and I think it deserves to be published in The Journal of Physical Chemistry Letters, but minor reversion is required.

#### Comments:

- 1. The authors used isothermal titration calorimetry to measure the Ag+ stoichiometry and affinity, and concluded that three handle-like silvers in the [C(4)C(5)C(6)]2 subduplex are Ag+, with the other 2 Ag+ in the neighbouring sub-structure, How can the authors clearly state the exact location of Ag+ only via titration results?
- 2. The author has problems with inconsistencies in all units in the manuscript and SI writing, for instance. kcal/mole Ag+ and cal/K mole Ag+, please corrected.
- 3. The silver salts should be detailed in the experimental section, as the reader cannot confirm whether the Ag+ species in the crystal growth section is the same as that used in the titration experiments.
- 4. The author used isotope exchange with D2O to make the deuterium scatters neutrons more efficiently than hydrogen, is there any incomplete substitution in above experiment due to the purity of D2O, which may affect the conclusions from the NSLD?
- 5. Some silver nanoclusters should be noted in revised version such as ACS Nano 2019, 13, 5753; J. Am. Chem. Soc. 2022, 144, 18305; Angew. Chem. Int. Ed., 61, (2022), e202200823

#### Reviewer: 2

#### Comments to the Author

In the manuscript by David et al., neutron scattering and calorimetry are applied to unravel detailed information of the presence or absence of hydrogens in the structure of a DNA-stabilized green emitting silver 8 cluster. While based to some extend on previous data presented in Huard et al. 2019 JACS, new

details emerged in this study. I find that these results, which confirm the X-ray data, and go beyond it (X-ray does not allow to probe hydrogens very well, while neutron scattering is more suitable for this) merit publication in J Phys Chem Lett. after some minor revisions to improve the clarity.

- 1. In the crystal state, the silver 8 cluster presented in this paper is stabilized by three DNA strands. This is not clearly enough discussed in the manuscript and can only be indirectly inferred from the \* in Figure 1D (and even there the meaning of the \* is not given). It should be clearly discussed in the manuscript that A(1)\*B is not from the two main dimer strands that are wrapped around the cluster. This adenine is responsible for interactions with two of the five trapezoidal atoms, which is a significant amount.
- 2. Related to the previous comment, how do the authors envision that this translate to the solution phase and the experiments with (A2C4)-teg-(iA2iC4). Would in this case A(1)B take over the role of A(1)\*B?
- 3. "Most importantly, NSLD maps suggest that the C6-NH2 and C4-NH2 coordinate silvers because they are singly deprotonated (Table 1)." It is not clear how the authors determined this. Is there a difference in intensity of the magenta spheres in Figure 1D? Or is this based on common sense that there is no space for a hydrogen at these positions? Please provide some information on how you came to this conclusion.

#### Reviewer: 3

#### Comments to the Author

The manuscript "Mapping H+ in the Nanoscale (A2C4)2-Ag8 Fluorophore" by David, et al., presents the first crystallographic study of DNA-stabilized silver nanoclusters using neutron scattering. The growth of DNA-Ag crystals to nearly millimeter size scales is an impressive achievement and makes possible for the first time to perform neutron scattering studies of a DNA-stabilized silver nanocluster species. These studies are important because neutron scattering, unlike X-ray scattering, can resolve the locations of hydrogen atoms. Thus, the major contribution of this study is its report of the protonation state of the DNA oligomer that stabilizes the silver nanocluster, as such information was not available previously and would be especially useful for computational groups studying these emerging nanoclusters.

In general, the reviewer finds this manuscript suitable for publication with minor revisions. One particular issue is the comparison of the unreduced Ag+-DNA solutions to the reduced nanocluster, which should be clarified. Specific comments and recommendations are numbered below.

- 1. Pg. 5 paragraph 1: Others have reported evidence of novel hydrogen bonding in DNA-silver duplexes beyond crystallographic studies, of relevance to the (A2C4)2-Ag8 studied here, and the reviewer recommends referencing these previous studies in 2017 and 2018. Chen, et al. reported evidence of such hydrogen bonds in cytosine-Ag+-cytosine duplexes ( DOI 10.1021/acsomega.7b01089), and Swasey, et al, reported evidence of novel hydrogen bonds in guanine-Ag+-guanine duplexes and possibly also cytosine-Ag+-cytosine duplexes (DOI 10.1021/acs.jpclett.8b02851). It would be helpful to readers to comment on how these additional past studies compare with the authors' findings.
- 2. Figure 1F: the reviewer notes that it is very difficult to intuit the 60° twist of the base pairs from this figure, which appears to show more planar base pairs than in Fig. 1C, D.

- 3. Pg 6: The authors state that the stoichiometry of 5 Ag+ per DNA duplex is relatively low, but this seems to agree well with past studies of DNA duplication by Ag+ by Swasey, et al (2014, DOI: 10.1038/srep10163). They reported that Ag+ mediated duplexes of cytosine homobase strands and that adenine homobase strands did not form silver-mediated duplexes but did associated with a few silvers. Could such adenine-silver association be responsible for some of the silver stoichiometry that the authors find by ITC, with the majority of the silvers mediating cytosine base pairs?
- 4. Pg 6: DNA-stabilized silver nanoclusters are typically formed by borohydride reduction of DNA-silver salt mixtures (as developed by the corresponding author of this manuscript). The ITC experiments are, of course, just measuring the association of silver cations and DNA, which is not the nanocluster itself. It would be interesting and helpful to remind the readers that these Ag+-DNA mixtures are precursors to the nanocluster and to comment on how similar the stoichiometry of the Ag+-DNA complexes is expected to be as compared to the reduced nanocluster. (Some readers may misunderstand that the ITC experiments are not performed on the nanocluster formation process.)
- 5. pg. 7: Can the authors comment on how the protonation state of the crystallized DNA-stabilized silver nanocluster is expected to compare to the solvated nanocluster? Does some protonation occur during crystallization to promote charge neutralization? Placing this question in context of what is known about other biomolecules' protonation states before and after the crystallization process would enhance this paper's impact.

6. pg 8-9: Again, the authors use calorimetry to estimate the oxidation state of the nanocluster, but DNA-stabilized silver nanoclusters are typically formed by borohydride reduction. The reviewer again brings up the question in Comment #4 - how relevant are the unreduced complexes for the composition of the formed nanoclusters?

Author's Response to Peer Review Comments:

11/18/2022

Professor Editor Senior Editor The Journal of Physical Chemistry Letters

Manuscript ID: jz-2022-0316k

Title: Mapping H<sup>+</sup> in the Nanoscale (A<sub>2</sub>C<sub>4</sub>)<sub>2</sub>-Ag<sub>8</sub> Fluorophore

Dear Professor Editor,

Thank you for considering a revised version of our manuscript for publication in *The Journal of Physical Chemistry Letters*. We are grateful for the comments of the reviewers. Below, detailed responses to their comments are provided. The page numbers refer to our revised manuscript with tracked changes that is also uploaded as "Supporting Information for Review Only". These files are <u>V17.docx</u> and <u>SupplementalFile NDA.docx</u>.

We appreciate your time and consideration of our manuscript.

Sincerely,

Jeffrey T. Petty

# Reviewer 1:

Reviewer Comment 1. The authors used isothermal titration calorimetry to measure the Ag+ stoichiometry and affinity, and concluded that three handle-like silvers in the [C(4)C(5)C(6)]2 subduplex are Ag+, with the other 2Ag+ in the neighbouring sub-structure, How can the authors clearly state the exact location of Ag+ only via titration results?

<u>Author Reply:</u> The motivation for studying the reaction of oxidized Ag<sup>+</sup> with DNA is explained.

**Revision (see Page 6):** This sub-duplex shares key structural features with other DNA complexes with oxidized silvers:  $Ag^+$ -DNA bond lengths of 2.1 - 2.2 Å, N-Ag<sup>+</sup>-N bond angles of 164- $176^\circ$ , and base pairs twisted by  $30^\circ$ - $60^\circ$ . Here, we consider thermodynamic similarities by reacting  $Ag^+$  with a  $A_2C_4$  duplex and measuring the  $Ag^+$  stoichiometry and affinity using isothermal titration calorimetry. This reaction was considered because silver cluster chromophores, such as the green emitting  $Ag_{10}^{6+}$  and the near infrared emitting  $Ag_{30}^{18+}$ , can be significantly oxidized. We consider that the  $Ag^+$  and  $Ag^0$  may be distinct components within a DNA-cluster complex. We consider that  $Ag^+$  and  $Ag^0$  may

<u>Reviewer Comment 2:</u> The author has problems with inconsistencies in all units in the manuscript and SI writing, for instance. kcal/mole Ag+ and cal/K mole Ag+, please corrected.

<u>Author Reply:</u> The paper now uses that format for the thermodynamic parameters used in References 49-50.

**Revision (see Page 7):** The affinity of 5.0 ( $\pm$  0.2) x 10<sup>6</sup> M(Ag<sup>+</sup>)<sup>-1</sup> and  $\Delta H = -15.5$  ( $\pm$  1.3) kJ/mole Ag<sup>+</sup> are consistent with the stability of other Ag<sup>+</sup>-cytosine complexes. <sup>49-50</sup> The  $\Delta S = -26.4$  ( $\pm$  3.3) J/K mole Ag<sup>+</sup> may reflect the assembly of the duplex, but other factors may contribute to this change. <sup>50</sup>

Reviewer Comment 3. The silver salts should be detailed in the experimental section, as the reader cannot confirm whether the Ag+ species in the crystal growth section is the same as that used in the titration experiments.

Author Reply: This change is made.

**Revision** (see Page 2, Supplemental File): The drops with a volume of 40  $\mu$ L containing 0.9 mM A<sub>2</sub>C<sub>4</sub>, 6.5 equivalents of AgNO<sub>3</sub>, and 375 mM cacodylate buffer at pH = 6.5 were equilibrated against a 750- $\mu$ L reservoir composed of 34 or 36 % MPD.

<u>Reviewer Comment 4:</u> The author used isotope exchange with D2O to make the deuterium scatters neutrons more efficiently than hydrogen, is there any incomplete substitution in above experiment due to the purity of D2O, which may affect the conclusions from the NSLD?

Author Reply: Our detailed procedure is described in the Supplemental Material.

# Revision (see Page 8 and Pages 2 and 3, Supplemental Material):

<u>Page 8, Manuscript:</u> Most importantly, NSLD maps suggest that the C6-NH<sub>2</sub> and C4-NH<sub>2</sub> coordinate silvers because they are singly deprotonated (Table 1 and Supplemental Material).

<u>Page 2, Supplemental:</u> Plugs of crystallization buffer prepared in D<sub>2</sub>O (99.9% D, Cambridge Isotopes) were inserted into both ends of the capillary. The capillary ends were then sealed with beeswax. The crystals were left to equilibrate for more than two months to exchange the hydrogen to deuterium via vapor exchange prior to neutron data collection. High D<sub>2</sub>O purity and extended vapor exchange period are important to achieve high H/D exchange level.

<u>Page 3, Supplemental:</u> Initially, we added deuterium and hydrogen atoms to the model refined against the X-ray data using phenix.ready set. Phenix.ready set uses the program REDUCE (Word, et al.(1999). J. Mol. Biol. 285, 1735-1747) to add hydrogen/deuterium atoms in standardized geometry. The model generated contained H and D atoms in 0.5:0.5 ratio and was refined against the neutron data. The NSLD maps and the refined H:D exchange ratios were then inspected. This approach led to two types of H/D sites: type 1) H/D atom pointing away from the Ag atoms with these positions having high D occupancy; and type 2) H/D atoms positioned between the exocyclic N6 or N4 and the Ag atoms with refined H:D ratio of ~0.65:0.35. While this later ratio is experimentally possible, it most often signals an absence of H/D atoms at the concerned position (i.e. deprotonation) because the scattering length of H (-3.74 fm) and the scattering length of D (+6.67 fm) cancel each other at that specific ratio. To avoid the uncertainty arising from H:D ratios in the model, we then generated only deuterium atoms at all the exchangeable position. Neutron scattering length density (NSLD) Polder maps were calculated for all exocyclic amino groups to determine the protonation state of the nitrogen atoms. 1 The nuclear density supported modeling of deuterium atoms with 100% occupancy at all the predicted position (Fig. 1) except for the exocyclic group of A(2) from strand B which was best modeled as 75%H/25%D. As discussed above, this ratio does not allow us to fully rule out that the C6-NH<sub>2</sub> A(2) from strand B is doubly deprotonated. However, there is no chemical rational to explain a fully deprotonated C6-NH<sub>2</sub> and therefore we conclude that exchange is limited at this site and that this N is singly deprotonated. Using this approach, no residual nuclear density was left, indicating that there was no deuterium between the N6 or N4 and the Ag atoms. In the crystal structure presented here, we observed the exocyclic amine group of A(1) of strand B to be singly deprotonated. This protonation state is likely due to the crystal packing which positions an Ag atom between this group and the N1 atom of a A(1) of symmetry related molecule. Refinement statistics for the X-ray and neutron models are shown in Table S1. The neutron model was deposited in the Protein Data Bank (ID: 8DYK).

\_\_\_\_\_

Reviewer Comment 5: Some silver nanoclusters should be noted in revised version such as ACS Nano 2019, 13, 5753; J. Am. Chem. Soc. 2022, 144, 18305; Angew. Chem. Int. Ed., 61, (2022), e202200823

<u>Author Reply:</u> The structure and fluorescence of other silver complexes is discussed. The suggested references are cited.

**Revision** (see Page 3): The structure of nanoscale silver complexes guides the rational synthesis of specific chromophores. <sup>15-17</sup> For the DNA-silver chromophores (A<sub>2</sub>C<sub>4</sub>)<sub>2</sub>-Ag<sub>8</sub> and (CACCTGCGA)<sub>2</sub>-Ag<sub>16</sub>, three types of bonds have been identified via atomic resolution structures. <sup>18-20</sup>

# Reviewer 2:

Reviewer Comment 1: In the crystal state, the silver 8 cluster presented in this paper is stabilized by three DNA strands. This is not clearly enough discussed in the manuscript and can only be indirectly inferred from the \* in Figure 1D (and even there the meaning of the \* is not given). It should be clearly discussed in the manuscript that A(1)\*B is not from the two main dimer strands that are wrapped around the cluster. This adenine is responsible for interactions with two of the five trapezoidal atoms, which is a significant amount.

Author Reply:  $A(1)_B$ \* is defined.

**Revision (see Page 6, Figure 2 Caption):** (D) Representation of the protonation states for A(1)A(2)C(3) in strand A and A(1)\*A(2)C(3) in strand B, where A(1)\* is from a neighboring, symmetry-related strand. And (Page 7, top): "This structure assumes that  $A(1)_B$ \* is an artifact of crystallization and can be substituted with the corresponding adenine within a single dimer (see Figure 1D and insert in Figure 2)".

Reviewer Comment 2: Related to the previous comment, how do the authors envision that this translate to the solution phase and the experiments with (A2C4)-teg-(iA2iC4). Would in this case A(1)B take over the role of A(1)\*B?

Author Reply: The role of the  $A(1)_B^*$  in the synthetic dimer is discussed.

**Revision** (see Page 7): This structure assumes that the shared  $A(1)_B^*$  in the crystal structure can be substituted with the corresponding adenine in the dimer (see Figure 1D and insert in Figure 2).

<u>Reviewer Comment 3:</u> "Most importantly, NSLD maps suggest that the C6-NH2 and C4-NH2 coordinate silvers because they are singly deprotonated (Table 1)." It is not clear how the authors determined this. Is there a difference in intensity of the magenta spheres in Figure 1D? Or is this based on common sense that there is no space for a hydrogen at these positions? Please provide some information on how you came to this conclusion.

Author Response: Our detailed procedure is described in the Supplemental Material.

### Revision (see Page 8 and Page 3, Supplemental Material):

<u>Page 8, Manuscript:</u> Most importantly, NSLD maps suggest that the C6-NH<sub>2</sub> and C4-NH<sub>2</sub> coordinate silvers because they are singly deprotonated (Table 1 and Supplemental Material).

Page 3, Supplemental: Initially, we added deuterium and hydrogen atoms to the model refined against the X-ray data using *phenix.ready set*. Phenix.ready set uses the program REDUCE (Word, et al.(1999). J. Mol. Biol. 285, 1735-1747) to add hydrogen/deuterium atoms in standardized geometry. The model generated contained H and D atoms in 0.5:0.5 ratio and was refined against the neutron data. The NSLD maps and the refined H:D exchange ratios were then inspected. This approach led to two types of H/D sites: type 1) H/D atom pointing away from the Ag atoms with these positions having high D occupancy; and type 2) H/D atoms positioned between the exocyclic N6 or N4 and the Ag atoms with refined H:D ratio of ~0.65:0.35. While this later ratio is experimentally possible, it most often signals an absence of H/D atoms at the concerned position (i.e. deprotonation) because the scattering length of H (-3.74 fm) and the scattering length of D (+6.67 fm) cancel each other at that specific ratio. To avoid the uncertainty arising from H:D ratios in the model, we then generated only deuterium atoms at all the exchangeable position. Neutron scattering length density (NSLD) Polder maps were calculated for all exocyclic amino groups to determine the protonation state of the nitrogen atoms. The nuclear density supported modeling of deuterium atoms with 100% occupancy at all the predicted position (Fig. 1) except for the exocyclic group of A(2) from strand B which was best modeled as 75%H/25%D. As discussed above, this ratio does not allow us to fully rule out that the C6-NH<sub>2</sub> A(2) from strand B is doubly deprotonated. However, there is no chemical rational to explain a fully deprotonated C6-NH<sub>2</sub> and therefore we conclude that exchange is limited at this site and that this N is singly deprotonated. Using this approach, no residual nuclear density was left, indicating that there was no deuterium between the N6 or N4 and the Ag atoms. In the crystal structure presented here, we observed the exocyclic amine group of A(1) of strand B to be singly deprotonated. This protonation state is likely due to the crystal packing which positions an Ag atom between this group and the N1 atom of a A(1) of symmetry related molecule.

# Reviewer 3:

Reviewer Comment 1: Pg. 5 paragraph 1: Others have reported evidence of novel hydrogen bonding in DNA-silver duplexes beyond crystallographic studies, of relevance to the (A2C4)2-Ag8 studied here, and the reviewer recommends referencing these previous studies in 2017 and 2018. Chen, et al. reported evidence of such hydrogen bonds in cytosine-Ag+-cytosine duplexes (DOI 10.1021/acsomega.7b01089), and Swasey, et al, reported evidence of novel hydrogen bonds in guanine-Ag+-guanine duplexes and possibly also cytosine-Ag+-cytosine duplexes (DOI 10.1021/acs.jpclett.8b02851). It would be helpful to readers to comment on how these additional past studies compare with the authors' findings.

Author Reply: Silver and hydrogen bonding in other DNA-silver complexes is discussed.

**Revision** (see Page 5): Collective interactions of silvers and hydrogens with nucleobases have also be identified in related complexes using mass spectrometry, spectroscopic, and calorimetry/structural studies. 36-37 For example, cytosine strands form duplexes whose strands are linked via both Ag<sup>+</sup> with inter- and intra-nucleobase hydrogen bonds. 38-39 These interactions open new paths to DNA nanostructures and nanomachines.<sup>40</sup>

Reviewer Comment 2: Figure 1F: the reviewer notes that it is very difficult to intuit the 60° twist of the

base pairs from this figure, which appears to show more planar base pairs than in Fig. 1C, D.

Author Reply: The propeller twisting is now indicated in the 3-d model in Figure 1C.

**Revision** (see Page 6): Figure 1 has been modified.

Reviewer Comment 3: Pg 6: The authors state that the stoichiometry of 5 Ag+ per DNA duplex is relatively low, but this seems to agree well with past studies of DNA duplication by Ag+ by Swasey, et al (2014, DOI: 10.1038/srep10163). They reported that Ag+ mediated duplexes of cytosine homobase strands and that adenine homobase strands did not form silver-mediated duplexes but did associated with a few silvers. Could such adenine-silver association be responsible for some of the silver stoichiometry that the authors find by ITC, with the majority of the silvers mediating cytosine base pairs?

Author Response: Nucleobase crosslinking in other complexes is discussed. Ag<sup>+</sup> association with the adenines in the neighboring substructure is discussed.

**Revision** (see Page 7): The stoichiometry of  $5.0 \pm 0.2 \,\mathrm{Ag^+/(A_2C_4)_2}$  duplex is larger than the 12 nucleobases in this strand, so we propose that the duplex folds and is crosslinked by Ag<sup>+</sup> adducts, as observed in the crystal structure and in other complexes (Figures 1A/B). 36-37

The other 2 Ag<sup>+</sup> may be part of the neighboring sub-structure of this complex.

Reviewer Comment 4: Pg 6: DNA-stabilized silver nanoclusters are typically formed by borohydride reduction of DNA-silver salt mixtures (as developed by the corresponding author of this manuscript). The ITC experiments are, of course, just measuring the association of silver cations and DNA, which is not the nanocluster itself. It would be interesting and helpful to remind the readers that these Ag+-DNA mixtures are precursors to the nanocluster and to comment on how similar the stoichiometry of the Ag+-DNA complexes is expected to be as compared to the reduced nanocluster. (Some readers may misunderstand that the ITC experiments are not performed on the nanocluster formation process.)

Author Response: The motivation for studying the reaction of oxidized Ag<sup>+</sup> with DNA is explained.

**Revision (see Page 6):** This sub-duplex shares key structural features with other DNA complexes with oxidized silvers:  $Ag^+$ -DNA bond lengths of 2.1-2.2 Å, N-Ag<sup>+</sup>-N bond angles of 164- $176^\circ$ , and base pairs twisted by  $30^\circ$ - $60^\circ$ . Here, we consider thermodynamic similarities by reacting  $Ag^+$  with a  $A_2C_4$  duplex and measuring the  $Ag^+$  stoichiometry and affinity using isothermal titration calorimetry. This reaction was considered because silver cluster chromophores, such as the green emitting  $Ag_{10}^{6+}$  and the near infrared emitting  $Ag_{30}^{18+}$ , can be significantly oxidized. We consider that the  $Ag^+$  and  $Ag^0$  may be distinct components within a DNA-cluster complex.

Reviewer Comment 5: pg. 7: Can the authors comment on how the protonation state of the crystallized DNA-stabilized silver nanocluster is expected to compare to the solvated nanocluster? Does some protonation occur during crystallization to promote charge neutralization? Placing this question in context of what is known about other biomolecules' protonation states before and after the crystallization process would enhance this paper's impact.

<u>Author Response</u>: The pH at which crystals are grown rather than the process of crystallization itself impacts the observed protonation states in crystallographic structures. We further discuss interfacial factors in the Supplemental Material.

### Revision (see Pages 2 and 3, Supplemental Material):

<u>Page 2, Supplemental:</u> Plugs of crystallization buffer prepared in D<sub>2</sub>O (99.9% D, Cambridge Isotopes) were inserted into both ends of the capillary. The capillary ends were then sealed with beeswax. The crystals were left to equilibrate for more than two months to exchange the hydrogen to deuterium via vapor exchange prior to neutron data collection. High D<sub>2</sub>O purity and extended vapor exchange period are important to achieve high H/D exchange level.

<u>Page 3, Supplemental:</u> This protonation state is likely due to the crystal packing which positions an Ag atom between this group and the N1 atom of a A(1) of symmetry related molecule

Reviewer Comment 6: pg 8-9: Again, the authors use calorimetry to estimate the oxidation state of the nanocluster, but DNA-stabilized silver nanoclusters are typically formed by borohydride reduction. The reviewer again brings up the question in Comment #4 - how relevant are the unreduced complexes for the composition of the formed nanoclusters?

<u>Author Response:</u> The motivation for studying the reaction of oxidized Ag<sup>+</sup> with DNA is explained.

**Revision (see Page 6):** This sub-duplex shares key structural features with other DNA complexes with oxidized silvers:  $Ag^+$ -DNA bond lengths of 2.1-2.2 Å, N-Ag<sup>+</sup>-N bond angles of 164- $176^\circ$ , and base pairs twisted by  $30^\circ$ - $60^\circ$ . Here, we consider thermodynamic similarities by reacting  $Ag^+$  with a  $A_2C_4$  duplex and measuring the  $Ag^+$  stoichiometry and affinity using isothermal titration calorimetry. This reaction was considered because silver cluster chromophores, such as the green emitting  $Ag_{10}^{6+}$  and the near infrared emitting  $Ag_{30}^{18+}$ , can be significantly oxidized. We consider that the  $Ag^+$  and  $Ag^0$  may be distinct components within a DNA-cluster complex. We

# **Editorial Office**

Comment 1: Please include country in all of the author affiliations in the publication file(s).

Author Reply: These changes have been made on Pages 1.

\_\_\_\_\_

<u>Comment 2:</u> Please add full header at top of page of the Supporting Information file, which includes: Title (in title case), Full Author List, and Author affiliations (exactly as they appear in the manuscript).

<u>Author Reply:</u> These changes have been made on Page 1 of the revised Supplemental File.

\_\_\_\_\_

Comment 3: In both the main file and the supporting information, fix the style of all references to use JPCL formatting (check all references carefully). \*\*\*JPC Letters reference formatting requires that journal references should contain: () around numbers, author names, article title (titles entirely in title case or entirely in lower case), abbreviated journal title (italicized), year (bolded), volume (italicized), and pages (first-last). Book references should contain author names, book title (in the same pattern), publisher, city, and year. Websites must include date of access.

<u>Author Reply:</u> These changes have been made in the References.